

OVERVIEW OF THE LASER WAKEFIELD ACCELERATION RESEARCH AT KERI

H. Suk*, C.B. Kim, G.H. Kim, J.U. Kim, KERI, Changwon, Korea,
 I.S. Ko, J.C. Kim, Department of Physics, POSTECH, Pohang, Korea,
 S.J. Hahn, Department of Physics, Chung-Ang University, Seoul, Korea, and
 W.B. Mori, Department of Physics, UCLA, Los Angeles, CA 90095, USA

Abstract

An overview of the ongoing advanced accelerator research at KERI is given, of which the research uses a T^3 (table-top terawatt) laser and plasma to generate an ultra-strong electric field for particle acceleration. The ongoing advanced accelerator research includes the self-trapping and acceleration of background plasma electrons in a sharp downward density transition, self-modulated laser wakefield acceleration, photon acceleration, and ion acceleration. In this paper, recent research results and future plans are presented.

1 INTRODUCTION

Scientists have studied to develop 1-TeV-level next generation linear colliders. If present RF-based accelerator technologies are used, the acceleration gradient is limited to less than 100 MeV/m at most so that the linear colliders will be tens of kilometers long and they will be very costly. Hence, alternative acceleration methods have been explored to overcome the limit of conventional RF-based accelerators.

One of the alternative acceleration methods is to use plasmas as plasmas can support ultrastrong electric fields [1][2]. It is shown that the plasma wave can produce an electric field of $E_z[V/m] \sim 96\sqrt{n_0}[cm^{-1}]$, where n_0 is a plasma density. According to this result, for example, a plasma of $n_0 = 10^{18} cm^{-3}$ can generate an electric field on the order of 100 GV/m, which is at least three orders of magnitude higher than that of RF-based conventional accelerators. Such an ultrastrong electric field can be generated by a plasma wave that can be produced by several different methods [3][4]. Since the so called CPA (Chirped-Pulse Amplification) technique [5] was invented in 1988, table-top terawatt lasers have been developed rapidly. Hence, nowadays compact and relatively low cost, but multiterawatt lasers are available and they can be used to excite a plasma wave known as a laser wakefield (LWF). If the multiterawatt laser pulse is focused in a plasma, an intensity of $I > 10^{18} W/cm^2$ is achieved and in this case plasma electrons are forced to move relativistically. If the pulse length $c\tau$ is approximately equal to the plasma wavelength λ_p , a relativistic LWF is generated efficiently and the resulting strong electric field can be used for charged particle acceleration.

Last year we launched an advanced accelerator research program using lasers and plasmas at Korea Electrotechnology Research Institute (KERI). The ongoing research topics include self-trapping and acceleration of background plasma electrons in a sharp downward density transition, self-modulated laser wakefield acceleration (SM-LWFA) [6][7], photon acceleration [8], and ion acceleration. In this paper, an overview of the present research activities at KERI is given and future plans are presented.

2 TRAPPING OF PLASMA ELECTRONS AT A DENSITY TRANSITION

In order to accelerate electrons with a LWF, particles should be injected into the acceleration phase of a wakefield. The injection can be done with several methods. For example, an injection accelerator or laser beams [9][10] can be used for injection. Another way is self-injection methods that do not require any external accelerator or laser beams. One of the self-injection methods is to send a plasma wave through a sharp downward density transition so that some background plasma electrons are trapped by the LWF due to the sudden increase in λ_p at the density transition. This idea [11] was originally proposed for an electron beam driver propagating in an underdense plasma (plasma density $n_0 < \text{beam density } n_b$), but it is believed that a similar trapping phenomenon would happen for a laser beam driver if the laser intensity is high enough. As mentioned above, compact T^3 lasers are available nowadays and they have more flexibilities than accelerators. Hence, it would be better if an electron beam driver is replaced by an intense laser pulse. In this section, the self-trapping method with a laser is investigated.

2.1 2-Dimensional Laser-Plasma Simulations

In order to study the trapping phenomenon, 2-dimensional (2-D) particle-in-cell (PIC) simulation studies have been performed. For the simulations we used the 2-D OSIRIS code [12] that was developed by the UCLA group.

In the simulation, the moving window has 1800 by 200 grids with 1.44 million particles and the plasma has a downward density transition from $5 \times 10^{18} cm^{-3}$ to $3 \times 10^{18} cm^{-3}$. Figure 1 shows the simulation result, which is a phase space plot (r, z) of the plasma electrons and the laser wake wave is moving to the right direction in the figure. Figure 1(a) shows the phase space plot when the laser wake

*hysuk@keri.re.kr

wave is passing the density transition. In the figure, some high density electrons are being separated from the first node of the wave. As time goes on, the electrons are completely separated from other electrons and they are self-injected into the acceleration phase of the laser wakefield (see Fig. 1(b)). The trapped electrons are accelerated to a high energy by the ultrastrong electric field which leads to an acceleration gradient of $dE/dz > 10$ GeV/m. In addition to acceleration, the trapped particles are observed to be strongly focused transversely by the background ions.

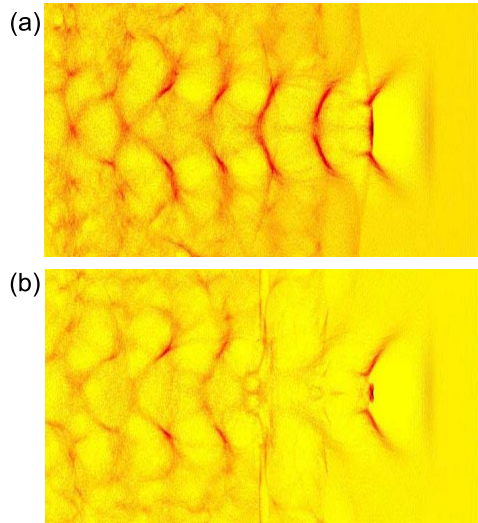


Figure 1: Phase space plot (r, z) of plasma electrons (a) when the laser wake wave is just passing the downward density transition and (b) when the laser wake wave just passed the density transition.

As the laser wake field continues to propagate, the trapped particles are further accelerated to a higher energy. Figure 2 shows a momentum phase space plot (p_z, z) of the plasma electrons, where the trapped plasma electrons gained energies between 5 MeV and 50 MeV. The energy can be increased further, but it should be pointed out that there is a limit in gaining the energy. Several effects can lead to the energy limit. One is the dephasing effect that is caused by the velocity difference between the laser wake field and the trapped electrons. As well known, a laser wakefield propagates at the speed of $v \simeq c\sqrt{1 - (\omega_p/\omega_0)^2} < c$ in a plasma, where c is the velocity of light in free space, ω_p and ω_0 are plasma and laser frequencies, respectively. Hence, the wake field velocity becomes smaller than that of highly relativistic electrons. As a result, the trapped electrons are gradually out of phase and they are not accelerated any more. Another important factor in energy saturation is the diffraction effect of a laser beam, which limits the interaction distance between the laser wakefield and the trapped electrons to the order of $2L_R = 2\pi r_0^2/\lambda_0$. Here, L_R is the Rayleigh range, r_0 is the laser beam radius, and λ_0 is the laser wavelength. In most cases, the diffraction effect is a dominant factor in energy saturation, but to some extent it can be compensated

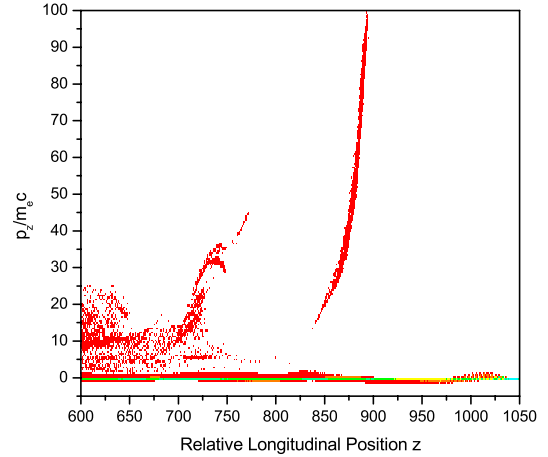


Figure 2: Momentum phase space plot (p_z, z) of the plasma electrons after the laser wake wave passed the downward density transition. Note that the major particles are trapped by the first period of a wakefield.

by a focusing effect that is caused by the relativistic motion of plasma electrons or by a parabolic-like plasma density profile. If the so called optical guiding [13] is employed, the interaction range of the laser wakefield and the trapped electrons can be considerably extended, so the energy gain can become much higher.

So far the simulations were performed for the density scale length $L_s = 0$, which implies that the density transition is infinitely sharp. However, this is not realistic. Hence, simulations were conducted for a finite density scale length to investigate the effect. The result is shown in Fig. 3, which indicates that the trapped charge Q is reduced gradually as the density scale length increases. When L_s/λ_p^{II} reaches 1, the trapped charge is reduced about 50%.

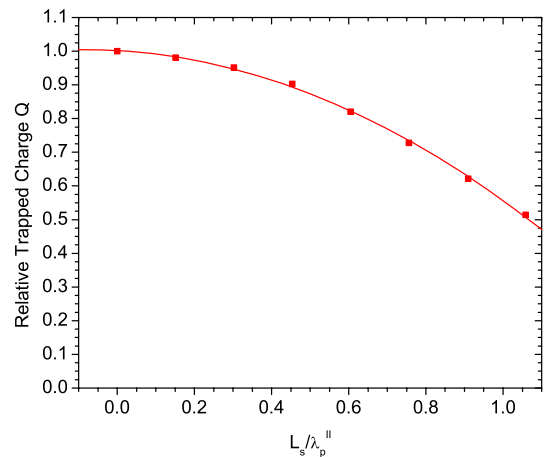


Figure 3: Relative trapped charge Q vs. L_s/λ_p^{II} , where λ_p^{II} is the laser wakefield wavelength in the low density side of a density transition.

2.2 Planned Experiment

In order to verify the self-trapping phenomenon, we plan to conduct experiments. In the above simulations, rather high plasma densities on the order of 10^{18} cm^{-3} were used, but using high densities was just to reduce the calculation time. In experiments, however, significantly lower density plasmas ($\sim 10^{16} \text{ cm}^{-3}$) will be used as lower densities will mitigate the requirement for sharpness in density transition. Furthermore, more particles are expected to be trapped for lower densities because the trapped charge is scaled as $Q \propto 1/\sqrt{n_0}$.

For the experiments, the 2 TW T^3 laser at Center for Advanced Accelerators of KERI, which is a Ti:sapphire/Nd:glass hybrid CPA laser, will be used. Figure 4 shows the 2 TW laser system that we have. In the figure, short laser pulses with a duration of about 150 fs are generated by the mode-locked Nd:glass oscillator and they are stretched in time by two gratings. And then, they are sent into the Ti:sapphire regenerative amplifier for energy amplification to about 0.5 mJ/pulse. The amplified laser pulse is sent to the final glass amplifier, which increases the energy to more than 2 J/pulse. The high energy, but long pulse laser beam is then compressed to less than 700 fs by gratings in the pulse compressor. The compressed short laser pulse has an output power of about 2 TW and this is sent into the laser-plasma interaction chamber. The laser beam will be focused to a small spot with a radius of about $21 \mu\text{m}$ in He gas. In this case, the laser intensity I will exceed $3 \times 10^{17} \text{ W/cm}^2$ and a laser-produced plasma will be generated. The gas density is adjusted in such a way that the laser wake wave has a wavelength of $\lambda_p^{II} = 210 \mu\text{m}$ as a wake wave can be efficiently excited for $\lambda_p \simeq c\tau$. Under these conditions the acceleration gradient dE/dz is expected to be a few GeV/m.

Generating a sharp density transition is critically important for the self-trapping experiment. To achieve the goal several different approaches will be tried. One of them could be to use a thin foil for gas separation. If the foil is thin enough, this method may work and high-energy electron beams are expected to be produced. Several important parameters of the beams, such as charge, energy, energy spread, emittance, beam size, etc., will be measured by various tools that include a Faraday cup, dipole magnet, emittance meter, OTR (Optical Transition Radiation), respectively. According to the simulation result and scaling laws, the self-trapping is expected to yield a significant amount of self-trapping in the range of tens of pC for $n_0 \sim 10^{16} \text{ cm}^{-3}$.

At present, preparations for this experiment are under way at Center for Advanced Accelerators of KERI. A new laser laboratory was built recently in a clean room (class 10,000) and installation of the T^3 laser system is scheduled to be finished by October, 2002. After laser beam characterizations, the self-trapping experiment at a density transition and the self-modulated laser wakefield experiment will be performed first.

Table 1: Designed experimental parameters.

Laser power P	$> 2 \text{ TW}$
Laser pulse duration τ	$< 700 \text{ fs}$
Laser wavelength λ_0	$1.053 \mu\text{m}$
Laser beam radius σ_r	$21 \mu\text{m}$
Rayleigh range L_R	1.3 mm
Laser intensity I	$> 3 \times 10^{17} \text{ W/cm}^2$
Plasma densities :	$n_0^I = 3.4 \times 10^{16} \text{ cm}^{-3}$
	$n_0^{II} = 2.5 \times 10^{16} \text{ cm}^{-3}$
Plasma wavelength λ_p^{II}	$210 \mu\text{m}$
Acceleration gradient dE/dz	a few GeV/m

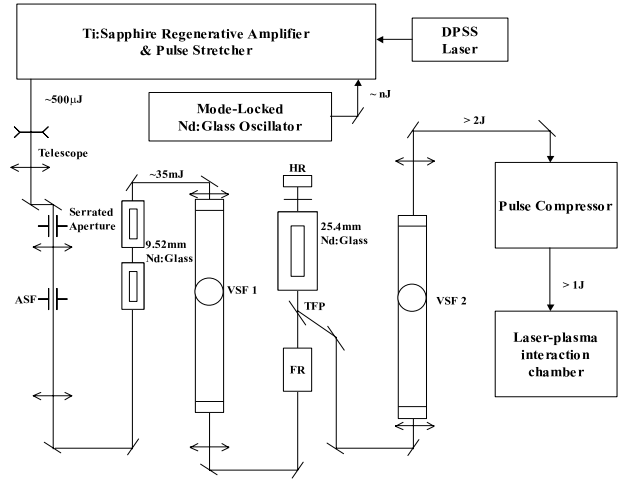


Figure 4: Layout of the 2 TW Ti:sapphire/Nd:glass laser system at Center for Advanced Accelerators of KERI.

3 SELF-MODULATED LASER WAKEFIELD ACCELERATION

When an intense laser beam with a long pulse length $c\tau \gg \lambda_p$ propagates in an underdense plasma ($\omega_p < \omega_0$), the laser beam (ω_0, k_0) decays into a plasma wave (ω_p, k_p) and forward-propagating laser light ($\omega_0 - \omega_p, k_0 - k_p$) due to the Raman scattering instability. As a result, the long laser pulse is split into many laser pulses with a period of λ_p . The self-modulated laser pulse train then excites the laser wake wave resonantly. When the self-modulated laser wakefield is generated, some background plasma electrons are self-injected into the acceleration phase. This is caused by some hot electrons that result from the Raman scattering instability, transverse or longitudinal wave breakings, etc. The self-injected electrons are then trapped by the self-modulated laser wakefield and accelerated to a high energy. In this case, however, the injection is randomly done in the acceleration phase. Therefore, the energy spread is naturally almost 100 %. Energy gain in the self-modulated laser wakefield acceleration is dominated by diffraction of the laser beam unless the relativistic self-focusing occurs. If the laser beam is strong enough, the laser is self-focused

due to the relativistic effect and in this case the energy can be increased significantly.

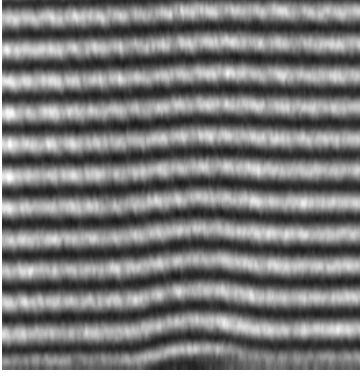


Figure 5: Interference pattern from the Mach-Zehnder interferometer when a He gas is ejected from the gas nozzle. In the figure, the He gas jet is flowing upward from the round nozzle with a diameter of $500 \mu\text{m}$ and the backing pressure is 50 bars.

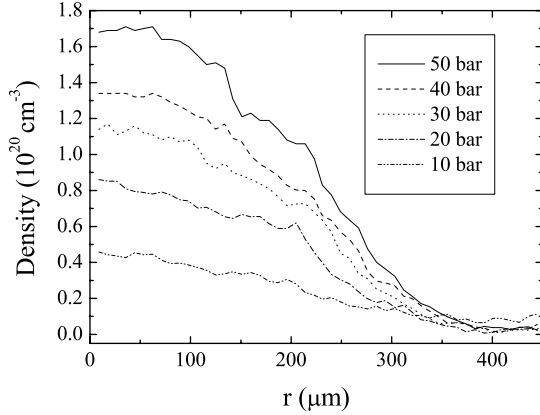


Figure 6: Density profile across the gas nozzle for different backing pressures.

At Center for Advanced Accelerators of KERI, we have an experimental plan for the SM-LWFA. For the experiment, a few gas nozzles were developed and tested. Test result of one nozzle is in Fig. 5, which shows an interference pattern of a He gas jet from a Mach-Zehnder interferometer. In the figure, the gas jet is moving upward and the fringe patterns are observed to be shifted. The shifted fringes can be analyzed to obtain a density profile and the result is shown in Fig. 6. The figure indicates that the density profile across the nozzle is almost Gaussian. In experiment, a gas density in the range of 10^{19} cm^{-3} will be used. Compared to a Gaussian-like density profile, a flat profile is better, so development of a long rectangular nozzle is under way and it is expected to give a better result. The experiment will be conducted with the 2 TW Ti:sapphire/Nd:glass hybrid laser system at KERI in 2003.

The 2 TW may not be high enough for efficient particle acceleration. In this case, another SM-LWFA experiment will be performed at K-JIST that will have a few tens of TW Ti:sapphire laser system by the end of 2003.

4 PHOTON ACCELERATION

The speed of light is constant in vacuum but it is possible to increase or decrease the speed of photons by using a medium which has nonuniform index of refraction. For a nonuniform plasma, the dispersion relation of an electromagnetic wave is

$$\omega^2(k; x, t) = \omega_p^2(x, t) + c^2 k^2, \quad (1)$$

where $\omega_p \equiv (n_0 e^2 / m \epsilon_0)^{1/2}$ is the electron plasma frequency and k is the wave number. Here, e , m_e , and ϵ_0 are the electron charge, electron mass, and permittivity in vacuum, respectively. If a laser pulse is located on a downward density gradient, the phase velocity at the front of the pulse is slower than that at the tail from Eq. (1), and thus the wavelength becomes short and the frequency is upshifted. Finally, the group velocity increases, and this phenomenon is called photon acceleration [8].

The interaction length between the laser pulse and the density gradient can be extended significantly by using a wake field generated by a short drive pulse. A probe pulse is launched with a time delay following the high intensity drive pulse propagating through a plasma. The interaction is most effective when the group velocity of the probe pulse is same as the phase velocity of the plasma wave generated by the drive. For this purpose, the frequency of the probe and the drive pulses are set to be same ω_0 . The plasma density n_0 is assumed to be uniform with a plasma frequency ω_{p0} . The wavelength of the plasma wave is $\lambda_{p0} = 2\pi c / \omega_{p0}$. When the driven plasma motion is not highly relativistic, the density perturbation δn shows a sinusoidal shape and increases with the increasing drive pulse intensity. From the dispersion relation of electromagnetic waves propagating through plasmas, the maximum frequency shift is calculated as [14]

$$\frac{\Delta\omega}{\omega_0} = \pi \frac{\omega_{p0}^2}{\omega_0^2} \frac{\delta n_0}{n_0} \frac{v_g T}{\lambda_{p0}}, \quad (2)$$

where v_g , T are the group velocity of the probe pulse and the propagation time, respectively. With this mechanism, it is possible to vary the laser wavelength continuously within the frequency upshift limit by changing the interaction length, $v_g T$.

We simulated photon acceleration using the one-dimensional (1-D) electromagnetic particle-in-cell code, 1-D XOOPIC [15], and 2-D OSIRIS code. Figure 7 shows a 1-D simulation result in which about 40% of frequency upshift was observed after 2.0 cm of interaction length. The used parameters are $n_0 = 10^{18} \text{ cm}^{-3}$ corresponding to $\lambda_{p0} = 33 \mu\text{m}$ and drive laser intensity of $1.18 \times 10^{18} \text{ W/cm}^2$ corresponding to the normalized vector potential

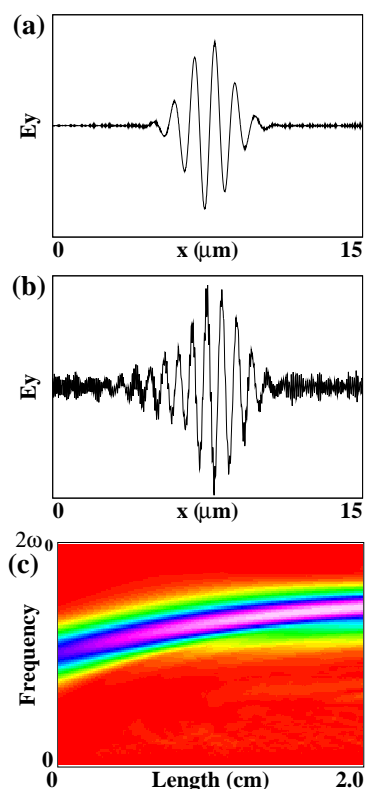


Figure 7: One-dimensional simulation results : (a) the pulse shape at the initial time, (b) the pulse shape when the interaction length is 2 cm, and (c) contour plot of frequency vs. interaction length.

$a_0 \equiv eE_y/mc\omega_0 = 1.0$. Moreover, 150% of frequency upshift was observed with an increased intensity of the drive pulse, $a_0 = 2.0$. In 1-D simulation, however, diffraction of the laser pulses is not considered and thus the interaction length is much longer than that of real situation. In 2-D simulations with the OSIRIS code, it was observed that photon acceleration saturates at smaller interaction length with only 10% of frequency upshift because of laser pulse diffraction and the transverse plasma motion.

There are saturation mechanisms of photon acceleration such as diffraction, wave dispersion, drive pulse depletion, and dephasing between the probe pulse and the plasma wake field. As shown in Eq. (2), the frequency upshift is effective for large n_0 and a_0 . However, they have limitations because the probe pulse disperses when the scale length of the density gradient is shorter than the pulse length of the probe. The density gradient becomes sharp and appears within a narrow region for large n_0 and a_0 . Moreover, if we decrease the laser spot size to increase the intensity of the drive pulse, the Rayleigh length decreases and the interaction length becomes shortened by diffraction. The interaction length, $v_g\tau$, is restricted to a few Rayleigh lengths by diffraction, and also restricted by the drive pulse depletion which gives its energy to plasma wake fields. Diffraction can be controlled by optical guiding of the laser us-

ing plasma channels. As the group velocity of the probe pulse increases by photon acceleration, the difference increases between the group velocity of the probe pulse and the phase velocity of the wake field. As the probe pulse is accelerated, it deviates from the acceleration phase. Dephasing can be controlled by changing the plasma density gradually as the pulse propagates.

5 CONCLUSIONS

Recent progress in advanced accelerator research is amazing. One of major reasons for such a remarkable progress may be attributed to the rapid progress in high power laser technologies. Nowadays terawatt table-top lasers are common around the world and they are used for laser and plasma-based advanced accelerator research. Such a T^3 laser system will be used for particle acceleration experiment at KERI, too. If the self-trapping scheme at a density transition is verified with a laser beam, it will be an important progress in advanced accelerator research. In addition, planned experiments for the SM-LWFA, ion acceleration, and recursive photon acceleration scheme for higher frequency upshift may lead to important results.

6 REFERENCES

- [1] T. Tajima and J. M. Dawson, Phys. Rev. Lett. **43**, 267 (1979).
- [2] C. Joshi, in *Proc. of the 9th Workshop on Advanced Accelerator Concepts* (AIP, New York, 2000), p. 85.
- [3] E. Esarey, P. Sprangle, J. Krall, and A. Ting, IEEE Trans. on Plasma Sci. **24**, 252 (1996).
- [4] D. Umstadter, Phys. Plasmas **8**, 1774 (2001).
- [5] P. Maine, D. Strickland, P. Bado, M. Pessot, and G. Mourou, IEEE J. Quantum Electron. **24**, 398 (1998).
- [6] K. Nakajima *et al.*, Phys. Rev. Lett. **74**, 4428 (1995).
- [7] C. Coverdale, C. B. Darrow, C. D. Decker, W. B. Mori, K. C. Tzeng, K. A. Marsh, C. E. Clayton, and C. Joshi, Phys. Rev. Lett. **74**, 4659 (1995).
- [8] S. C. Wilks, J. M. Dawson, W. B. Mori, T. Katsouleas, and M. E. Jones, Phys. Rev. Lett. **62**, 2600 (1989).
- [9] D. Umstadter, J. Kim, E. Dodd, Phys. Rev. Lett. **76**, 2073 (1996).
- [10] E. Esarey, R. F. Hubbard, W. P. Leemans, A. Ting, and P. Sprangle, Phys. Rev. Lett. **79**, 2682 (1997).
- [11] H. Suk, N. Barov, J. B. Rosenzweig, and E. Esarey, Phys. Rev. Lett. **86**, 1011 (2001).
- [12] R. G. Hemker, K. C. Tzeng, W. B. Mori, C. E. Clayton, and T. Katsouleas, Phys. Rev. E **57**, 5920 (1998).
- [13] P. Sprangle and B. Hafzi, Phys. Plasmas **6**, 1683 (1999).
- [14] E. Esarey, A. Ting, and P. Sprangle, Phys. Rev. A **42**, 3526 (1990).
- [15] H. J. Lee, P. J. Mardahl, G. Penn, and J. S. Wurtele, IEEE Trans. Plasma Science **30**, 40 (2002).